# 充滿非達西流體之多孔性介質在垂直渗透平板且具磁場之自然對流分析 Influence of non-Darcy on MHD-free convection over a vertical permeable plate in a porous medium

黄卓初 <sup>1</sup>空軍航空技術學院一般學科部飛機工程系

<sup>1</sup> Huang Chuo-Jeng
<sup>1</sup> Department of Aircraft Engineering, Air Force Institute of Technology

# 摘要

本文以一數值方法來分析熱質傳遞特性,在充滿非達西流體之飽和性多孔性介質在垂直滲透平板且具磁場之自然對流影響。垂直平板的表面為均勻壁溫度/均勻壁濃度。以凱勒盒子法來解轉換過的控制方程式。數值計算結果主要顯示浮力比N,路易士參數Le,非達西參數ND,磁場參數M和噴吸流參數ξ,對無因次溫度分佈、濃度分佈、局部Nusselt數和局部Sherwood數之影響,並將計算結果以圖表方式呈現。

關鍵字:熱質傳遞、非達西、磁場、垂直滲透板、多孔性介質

### **Abstract**

The heat and mass transfer characteristics of MHD-free convection about a vertical permeable flat plate embedded in a saturated porous medium is numerically analyzed. The surface of the vertical flat plate has a uniform wall temperature and uniform wall concentration (UWT/UWC). Non-similar solutions for the transformed governing equations by Keller box method are obtained. Numerical data for the dimensionless temperature profile, the dimensionless concentration profile, the local Nusselt number and the local Sherwood number are presented graphically for the buoyancy ratio N, the Lewis number Le, the non-Darcy parameter ND, the magnetic field parameter M and the blowing/suction parameter  $\xi$  which are entered in tables or plotted in figures.

Key word: heat and mass transfer, non-Darcy, MHD, vertical permeable plate, porous media

### 1. Introduction

The problem of magnetohydrodynamic flow (MHD-free convection) heat and mass transfer (or double-diffusion) about a flat plate in a saturated porous medium occur in many industrial or engineering applications such as the cooling of nuclear reactors, the geothermal system, petroleum industries, aerodynamic processes, and the heat exchanger design. Nield and Bejan [1] recently presented comprehensive account of the information in the field. Because of the wide application of the characteristic MHD-free convection in porous medium, it becomes one of the major topics of significant research in the last two centuries. Partha et al. [2] accounted for the Soret and Dufour effects in a non-Darcy porous medium. Chamkha and Ben-Nakhi [3] reported the MHD mixed convection—radiation interaction along a permeable surface immersed in a porous medium in the presence of Soret and Dufour's effects. Khalid et al. [4] presented the unsteady MHD free convection flow of Casson fluid past over an oscillating vertical plate embedded in a porous medium.

There are many scholars have been engaged in the free convection boundary-layer flows Darcy flow studies. It may be remarked that the Darcy law is valid for low-speed flow through porous media but for high-speed flow the non-Darcy law is found to be more

Regarding pure heat transfer, appropriate. Huenefeld [5] investigated the Plumb and non-Darcy natural convection from heated surfaces in saturated porous medium. El-Hakiem et al. [6] presented the combined heat and mass transfer on non-Darcy natural convection in a fluid saturated porous medium with thermophoresis. Murthy et al. [7] reported the double-diffusive free convection flow past an inclined plate embedded in a non-Darcy porous medium saturated with a nanofluid.

The objective of the present work is to extend the work of Partha et al. [2] to investigate the influence of non-Darcy on MHD-free convection over a vertical permeable plate in a porous medium. The governing equations have been solved numerically using Keller box method (KBM). The results are obtained for various values of the parameters.

# 2. Formulation and analysis

The considered problem is the influence of non-Darcy on MHD-free convection over a vertical permeable plate in a porous medium that the boundary condition is uniform wall temperature  $T_w$  and uniform wall concentration  $C_w$  (UWT/UWC), respectively. Consider a two-dimensional, steady, laminar flow of an incompressible electrically conducting fluid over a flat plate in the presence of a transverse magnetic field  $B_0$ , as shown in Fig. 1, while the induced magnetic field due to the motion of the electrically conducting fluid is negligible. The origin of the coordinate system is the leading edge of the vertical flat plate, where x and y are Cartesian coordinates for the distance along and normal to, respectively, the vertical flat plate surface.

All the fluid properties are assumed to be constant except for the density variation in the buoyancy term. Introducing the boundary layer and Boussinesq approximations, the governing equations and the boundary conditions based on the non-Darcy law can be written as follows:

Continuity equation:

$$\frac{\partial u}{\partial x} + \frac{\partial v}{\partial y} = 0 \tag{1}$$

Momentum (non-Darcy) equation:

$$\frac{c\sqrt{K}}{v} \cdot u^{2} + \left(\frac{K \cdot \sigma \cdot B_{0}^{2}}{\mu} + 1\right) \cdot u$$

$$= -\frac{K}{\mu} \left(\frac{\partial p}{\partial x} + \rho g\right) \tag{2}$$

$$\frac{c\sqrt{K}}{v} \cdot v^2 + v = -\frac{K}{\mu} \left( \frac{\partial p}{\partial y} \right) \tag{3}$$

Energy equation:

$$u\frac{\partial T}{\partial x} + v\frac{\partial T}{\partial y} = \alpha_m \frac{\partial^2 T}{\partial y^2} \tag{4}$$

Concentration equation:

$$u\frac{\partial C}{\partial x} + v\frac{\partial C}{\partial y} = D_m \frac{\partial^2 C}{\partial y^2}$$
 (5)

Boussinesq approximation:

$$\rho = \rho_{\infty} \left[ 1 - \beta_T (T - T_{\infty}) - \beta_C (C - C_{\infty}) \right] \tag{6}$$

**Boundary conditions:** 

$$y = 0: v = V_w, T = T_w, C = C_w$$
 (7)

$$y \to \infty$$
:  $u = 0$ ,  $T = T_{\infty}$ ,  $C = C_{\infty}$  (8)

Here, u and v are the Darcian velocities in the x- and y- directions, respectively; K is the permeability of the porous medium;  $\sigma$  is the electric conductivity of the fluid;  $B_0$  is the externally imposed magnetic field in y-direction; g is the acceleration due to gravity; p,  $\rho$ , and  $\mu$  are the pressure, the density and the absolute viscosity, respectively; and Care volume-averaged the temperature and concentration, respectively;  $\alpha_m$ and  $D_m$  are the equivalent thermal diffusivity and mass diffusivity, respectively;  $V_w$  is the uniform blowing/suction velocity.

The stream function  $\psi$  is defined by

$$u = \partial \psi / \partial y$$
 and  $v = -\partial \psi / \partial x$  (9)

Therefore, the continuity equation is automatically satisfied.

Next consider the Eqs. (2) and (3). Cross-differentiation  $\partial u/\partial y - \partial v/\partial x$ , eliminates the pressure terms in Eqs. (2) and (3). Further, by using the boundary layer approximation  $(\partial/\partial x << \partial/\partial y, v << u)$ , yields

$$\frac{c\sqrt{K}}{v} \cdot \frac{\partial u^{2}}{\partial y} + \left(\frac{K \cdot \sigma \cdot B_{o}^{2}}{\mu} + 1\right) \cdot \frac{\partial u}{\partial y}$$

$$= \frac{K \cdot g \cdot \rho_{\infty}}{\mu} \left(\beta_{T} \frac{\partial T}{\partial y} + \beta_{C} \frac{\partial C}{\partial y}\right)$$
(10)

Integrating equation (10) once and with the aid of equation (8), yields

$$\frac{c\sqrt{K}}{v} (u^{2}) + \left(\frac{K \cdot \sigma \cdot B_{0}^{2}}{\mu} + 1\right) \cdot u$$

$$= \left(\frac{K \cdot g \cdot \rho_{\infty}}{\mu}\right) \left[\beta_{T} (T - T_{\infty}) + \beta_{C} (C - C_{\infty})\right]$$
(11)

The following dimensionless variables are invoked:

$$\xi = \frac{2V_{w}x}{\alpha Ra^{\frac{1}{2}}} \tag{12.1}$$

$$\eta = \frac{y}{x} R a_x^{1/2} \tag{12.2}$$

$$f(\xi,\eta) = \frac{\psi}{\alpha R a_x^{\frac{1}{2}}}$$
 (12.3)

$$\theta(\xi,\eta) = \frac{T - T_{\infty}}{T_{w} - T_{\infty}} \tag{12.4}$$

$$\phi(\xi,\eta) = \frac{C - C_{\infty}}{C_{w} - C_{\infty}} \tag{12.5}$$

$$Ra_{x} = \frac{\rho_{\infty} \cdot g \cdot \beta_{T} \left[T_{w} - T_{\infty}\right] K}{\mu} \left(\frac{x}{\alpha}\right)$$
 (12.6)

where  $Ra_x$  is the local Rayleigh number.

Substituting Eqs. (12) into Eqs. (11), (4)-(5), (7)-(8) obtains

$$ND \cdot (f')^2 + (M+1) \cdot (f') = \theta + N \cdot \phi \tag{13}$$

$$\theta'' + \frac{1}{2}f \cdot \theta' = \frac{1}{2}\xi \left( f' \frac{\partial \theta}{\partial \xi} - \theta' \frac{\partial f}{\partial \xi} \right) \tag{14}$$

$$\frac{1}{Le}\phi'' + \frac{1}{2}f \cdot \phi' = \frac{1}{2}\xi \left(f'\frac{\partial\phi}{\partial\xi} - \phi'\frac{\partial f}{\partial\xi}\right) \tag{15}$$

The boundary conditions are defined as follows:

$$\eta = 0: f = -\frac{\xi}{2}, \ \theta = 1, \ \phi = 1$$
(16)

$$\eta \to \infty$$
:  $\theta = 0, \ \phi = 0$  (17)

For the new variables, the Darcian velocities in the x- and y- directions are also respectively obtained by

$$u = \frac{\alpha_m \cdot Ra_x}{x} \cdot f' \tag{18}$$

$$v = -\frac{\alpha_{m} \cdot R a_{x}^{1/2}}{x} \left[ \frac{1}{2} f + \frac{1}{2} \left( \xi \frac{\partial f}{\partial \xi} - \eta \cdot f' \right) \right]$$
 (19)

where primes denote differentiation with respect to  $\eta$ .  $\xi$  defined in Eq. (12.1) is the surface blowing/suction parameter; Eq. (16) can be obtained by integrating Eq. (19) versus  $\xi$  once and by setting  $\eta=0$  (at the surface, y=0, then  $\eta=0$ ), and with the help of boundary Eq. (7). On the one hand, for the case of blowing,  $V_w>0$  and hence  $\xi>0$ . On the other hand, for the case of suction,  $V_w<0$  and hence  $\xi<0$ . Besides, the non-Darcy parameter ND, the magnetic field parameter M, the buoyancy ratio N and the Lewis number Le are respectively defined as follows:

$$ND = \frac{c\sqrt{K}}{v} \cdot \frac{\alpha_m \cdot Ra_x}{x} \tag{20}$$

$$M = \frac{K \cdot \sigma \cdot B_0^2}{\mu} \tag{21}$$

$$N = \frac{\beta_c \left[ C_w - C_\infty \right]}{\beta_T \left[ T_w - T_\infty \right]}, \qquad Le = \frac{\alpha_m}{D_m}$$
 (22)

The results for heat and mass transfer rates have practical applications. The heat and mass transfer rates are expressed in terms of the local Nusselt number  $Nu_x$  and the local Sherwood number  $Sh_x$ , which are respectively defined as follows:

$$Nu_{x} = \frac{h_{x}x}{k} = \frac{q_{w}x}{\left[T_{w} - T_{\infty}\right]k} = \frac{-\left(\frac{\partial T}{\partial y}\right)_{y=0}x}{\left[T_{w} - T_{\infty}\right]}$$
(23)

$$Sh_{x} = \frac{h_{m,x}x}{D_{m}} = \frac{m_{w}x}{\left[C_{w} - C_{\infty}\right]D_{m}} = \frac{-\left(\frac{\partial C}{\partial y}\right)_{y=0}x}{\left[C_{w} - C_{\infty}\right]D_{m}}$$
(24)

By applying Eqs. (12) the local Nusselt number  $Nu_x$  and the local Sherwood number  $Sh_x$  in terms of  $Ra_x^{1/2}$  are respectively obtained by

$$\frac{Nu_{x}}{Ra_{x}^{1/2}} = -\theta'(\xi, 0) \tag{25}$$

$$\frac{Sh_{x}}{Ra_{x}^{1/2}} = -\phi'(\xi, 0) \tag{26}$$

### 3. Numerical method and validation

Equations (13)-(17) are integrating by combining the implicit finite difference approximation with the modified Keller box method of Cebeci and Bradshaw [8]. First, the partial differential converted into a system of five first-order equations. These first-order equations are then expressed in finite difference forms and solved along with their boundary conditions by applying an iterative scheme. This approach improves the convergence rate and the computation times.

Computations were performed with a personal computer with the first step size  $\Delta \xi = 0.1$  and  $\Delta \eta_i = 0.01$ . The variable grid parameter is chosen 1.01 and the value of  $\eta_{\infty} = 30$ . The iterative procedure is stopped to give the final temperature and concentration distributions when the error in computing the  $\theta'_{w}$  and  $\phi'_{w}$  in the next procedure becomes less than  $10^{-5}$ .

# 4. Results and Discussion

To validate the numerical method used, the heat and mass transfer results of the present results are compared to those of previously published papers. The accuracy of this method was verified by comparing the results with those of Chamkha and Ben-Nakhi [3], Plumb and Huenefeld [5] and Murthy et al. [7]. Table 1 lists the comparison of present results for various values of ND with  $N = \xi = M = 0$ . Table 2 lists the comparison of present results for various values of  $\xi$  with ND = N = M = 0. All values in Tables 1 to 2 list the comparisons showed excellent agreement with the numerical data in previous works. Table 3 lists the values of  $Nu_x/Ra_x^{1/2}$  and  $Sh_x/Ra_x^{1/2}$  for various values of ND, M,  $\xi$ , N and Le.

In this investigation, the problem of effect of non-Darcy and MHD coupled heat and mass transfer by free convection of a non-Newtonian fluid flow along a vertical permeable plate has been studied. Representative numerical results for the dimensionless temperature and concentration profiles and the local Nusselt and Sherwood numbers with the buoyancy ratio N=1, the Lewis number Le=2, the non-Darcy parameter ND ranging from 0 to 10, the magnetic field parameter M ranging from 0 to 4 and the blowing/suction parameter  $\xi$  ranging from -2 to 2 are shown in Figs. 2-4.

The effect of the magnetic field parameter M (M = 0, 1 and 4) on the dimensionless temperature profile and the dimensionless concentration profile with N=1, Le=2,  $\xi=-1$ and ND = 1. is plotted in Fig. 2, respectively. Inspecting of this figure shows that the dimensionless temperature profile and the dimensionless concentration profile decreases monotonically as the distance  $\eta$  from the plate increases. It is also observed that the increase of the magnetic field parameter M leads to a tendency to decrease the flow velocity; thus, dimensionless reducing both the wall  $-\theta'(\xi,0)$ temperature gradient and the dimensionless wall concentration  $-\phi'(\xi,0)$ . The analysis has shown that the dimensionless temperature and concentration profiles are significantly influenced by magnetic field parameter.

Table 4 lists the values of local Nusselt number  $Nu/Ra^{1/2}$  and the local Sherwood number  $Sh_x/Ra_x^{1/2}$  for various values of the magnetic field parameter M with N=1, Le = 2,  $\xi = -1$  and ND = 1. Generally, it has been observed that enhancing the magnetic field parameter M reduces both the local Nusselt number and the local Sherwood number. This is due to the fact that enhancing the magnetic field tends decreases parameter M to dimensionless surface temperature gradients and surface dimensionless concentration gradients, as shown in Fig. 2, thus lowering the local Nusselt number and the local Sherwood number.

Figure 3 portrays the dimensionless temperature and concentration profiles for three

values of the non-Darcy parameter ND (ND=0, 1 and 10) with N=1, Le=2, M=1,  $\xi=-1$ , respectively. The figure shows that the dimensionless temperature and concentration profiles decrease monotonically from the surface of the vertical flat plate to the ambient. Both the thermal boundary layer thickness  $\delta_T$  and the concentration boundary layer thickness  $\delta_C$  increase for the values of ND increase.

Table 5 lists the values of local Nusselt number  $Nu_x/Ra_x^{y^2}$  and the local Sherwood number  $Sh_x/Ra_x^{y^2}$  for various values of ND with N=1, Le=2, M=1 and  $\xi=-1$ . In general, it has been found that enhancing the non-Darcy parameter ND reduces both the local Nusselt number and the local Sherwood number. This is due to the fact that enhancing the non-Darcy parameter ND tends to decrease the dimensionless surface temperature gradients and the dimensionless surface concentration gradients, as shown in Fig. 3, thus lowering the local Nusselt number and the local Sherwood number.

Figure 4 portrays the dimensionless temperature and concentration profiles for three values of the blowing/suction parameter  $\xi$  $(\xi = -1, 0 \text{ and } 1) \text{ with } N = 1, Le = 2, M = 1,$ ND = 1, respectively. It has been found that the dimensionless temperature and concentration profiles decrease monotonically from the surface of the vertical flat plate to the ambient. Both the thermal boundary layer thickness  $\delta_{\tau}$ and the concentration boundary layer thickness  $\delta_{\scriptscriptstyle C}$  decrease for the case of suction. However, this trend reversed for the case of blowing. For suction case, it decreases the dimensionless temperature profiles  $\theta$  and the dimensionless concentration profiles  $\phi$ ; thus increases the dimensionless surface temperature gradient  $-\theta'(\xi,0)$ and the dimensionless surface concentration gradient  $-\phi'(\xi,0)$ . The analysis has shown that the dimensionless temperature and concentration profiles are appreciably influenced by blowing/suction parameter.

Table 6 lists the values of local Nusselt

number  $Nu_x/Ra_x^{y_2}$  and the local Sherwood number  $Sh_x/Ra_x^{y_2}$  for various values of  $\xi$  with N=1, Le=2, M=1 and ND=1. In general, it has been found that both the local Nusselt number and the local Sherwood number increase owing to the case of suction, i.e.,  $\xi < 0$ . This is because for the case of suction increases both the dimensionless surface temperature and concentration gradients, as shown in Fig. 4. With the aid of Eqs. (25)-(26), the larger the dimensionless surface temperature and concentration gradients, the greater the local Nusselt and Sherwood numbers.

### 5. Conclusions

A two-dimensional, laminar boundary layer analysis is presented to study the influence of non-Darcy and MHD on free convection of non-Newtonian fluids over a vertical permeable plate in a porous medium. After the coordinate transformation, the transformed governing equations are solved by Keller box method (KBM). Comparisons with previously published works show excellent agreement. Numerical solutions are obtained for different values of the non-Darcy parameter ND, the magnetic field the blowing/suction parameter and M parameter  $\xi$ . Results show that increasing the non-Darcy parameter ND or the magnetic field parameter M tends to reduce both the local Nusselt number and the local Sherwood number. In general, for the case of suction, both the local Nusselt number and the local Sherwood number increase. This trend reversed for blowing of fluid.

# References

- [1] D.A. Nield, A. Bejan, Convection in Porous Media, Springer-Verlag, New York, 2013.
- [2] M.K. Partha, P.V.S.N. Murthy, G.P. Raja Sekhar, Soret and Dufour effects in a non-Darcy porous medium, ASME Journal of Heat Transfer, Volume 128(6), Pages 605–610, 2006.
- [3] A.J. Chamkha, A. Ben-Nakhi, MHD mixed convection-radiation interaction along a

- permeable surface immersed in a porous medium in the presence of Soret and Dufour's effects, Heat and Mass Transfer, Volume 44, Pages 846–856, 2008.
- [4] A. Khalid, I. Khan, A. Khan, S. Shafie, Unsteady MHD free convection flow of Casson fluid past over an oscillating vertical plate embedded in a porous medium, Engineering Science and Technology, an International Journal, Volume 18(3), Pages 309–317, 2015.
- [5] O.A. Plumb, J.C. Huenefeld, Non-Darcy natural convection from heated surfaces in saturated porous medium, International Journal of Heat and Mass Transfer, Volume 24(4), Pages 765–768, 1981.
- [6] M.A. El-Hakiem, S.M. El-Kabeir, A.M. Rashad, Combined heat and mass transfer on non-Darcy natural convection in a fluid saturated porous medium with thermophoresis, International Journal of Applied Mechanics and Engineering, Volume 12(1), Pages 9–18, 2007.
- [7] P.V.S.N. Murthy, A. Sutradhar, Ch. RamReddy, Double-diffusive free convection flow past an inclined plate embedded in a non-Darcy porous medium saturated with a nanofluid, Transport in Porous Media, Volume 98(3), Pages 553–564, 2013.
- [8] T. Cebeci, P. Bradshaw, Physical and Computational Aspects of Convective Heat Transfer, Springer-Verlag, New York, 1984.

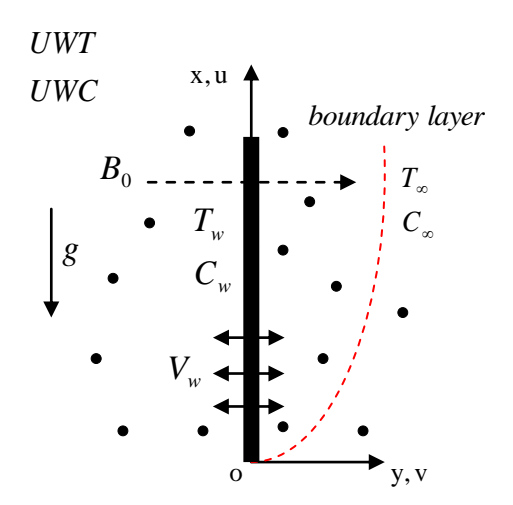
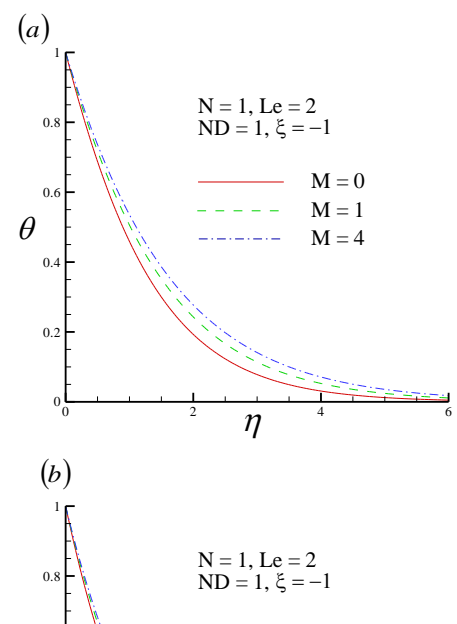


Fig. 1 The flow model and the physical coordinate system



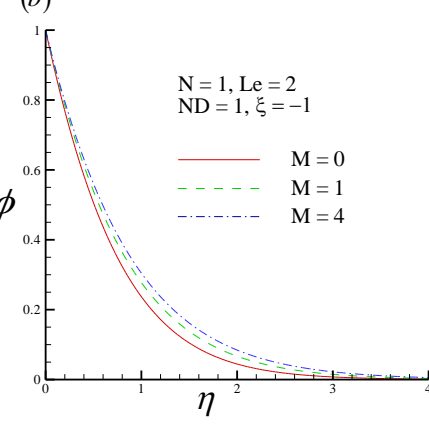
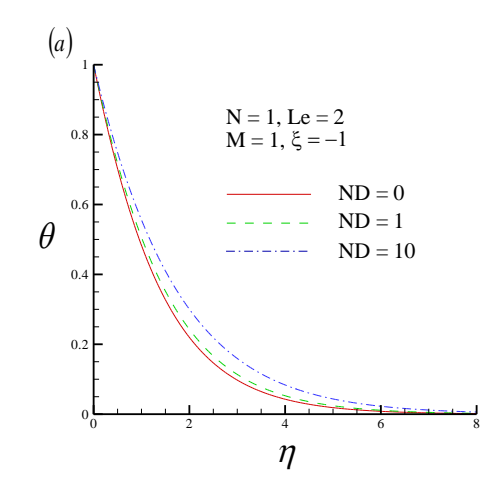


Fig. 2. (a) The dimensionless temperature profile and (b) the dimensionless concentration profile for three values of magnetic field parameter M.



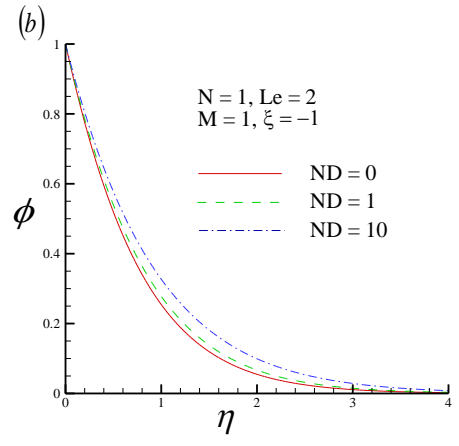
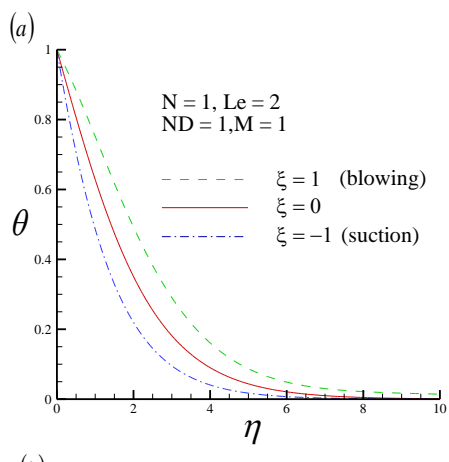


Fig. 3. (a) The dimensionless temperature profile and (b) the dimensionless concentration profile for three values of the non-Darcy parameter *ND*.



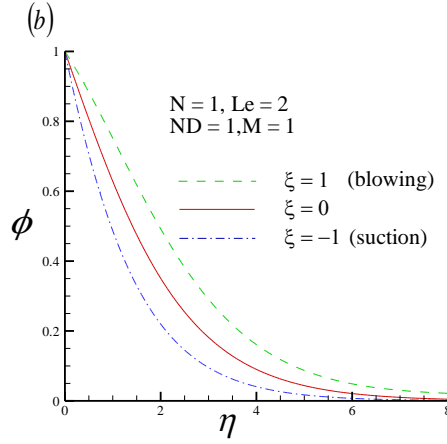


Fig. 4. (a) The dimensionless temperature profile and (b) the dimensionless concentration profile for three values of the blowing/suction parameter  $\xi$ .

Table 1. Comparison of present results for various values of *ND* with  $N = \xi = M = 0$ .

	$-\theta'(\xi,0)$			
ND	Plumb	Murthy		
	and	et al.	Present	
	Huenefeld	[7]	results	
	[5]	Γ, 1		
0.00	0.4439	0.4437	0.4437	
0.01	0.4423	0.4421	0.4421	
0.10	0.4296	0.4295	0.4295	
1.00	0.3661	0.3657	0.3657	
10.00	0.2512	0.2506	0.2506	
100.00	0.1518	0.1514	0.1514	

Table 2. Comparison of present results for various values of  $\xi$  with ND = N = M = 0.

	$-\theta'(\xi,0)$			
ξ	Chamkha and	Present		
	Ben-Nakhi [3]	results		
-4	1.9989	2.0014		
-2	1.0726	1.0725		
0	0.4440	0.4437		
2	0.1424	0.1407		
4	0.0340	0.0329		

Table 3. Values of  $Nu_x/Ra_x^{y/2}$  and  $Sh_x/Ra_x^{y/2}$  for various values of ND, M,  $\xi$ , N and Le.

ND	M	ξ	N	Le	$Nu_x / Ra_x^{1/2}$	$Sh_x/Ra_x^{1/2}$
0	0	0	1	2	0.5925	0.9295
1	0	0	1	2	0.4502	0.6916
0	1	0	1	2	0.4190	0.6572
0	0	1	1	2	0.4080	0.5454
0	0	-1	1	2	0.8383	1.4773
0	0	0	2	2	0.7097	1.1221
0	0	0	1	5	0.4437	1.1538

First row is baseline.

# 航空技術學院學報 第十七卷 第一期(民國一○七年)

Table 4. The values of  $Nu_x/Ra_x^{1/2}$  and  $Sh_x/Ra_x^{1/2}$  for various values of M with N=1, Le=2,  $\xi=-1$  and ND=1.

M	$Nu_x/Ra_x^{1/2n}$	$Sh_x/Ra_x^{1/2n}$
0.0	0.7136	1.2770
0.5	0.6739	1.2244
1.0	0.6430	1.1830
1.5	0.6187	1.1503
2.0	0.5994	1.1244

Table 5. The values of  $Nu_x/Ra_x^{1/2}$  and  $Sh_x/Ra_x^{1/2}$  for various values of ND with N=1, Le=2, M=1,  $\xi=-1$ .

ND	$Nu_x/Ra_x^{1/2}$	$Sh_x/Ra_x^{1/2}$
0.01	0.6788	1.2399
0.1	0.6740	1.2321
1	0.6430	1.1830
10	0.5692	1.0769
100	0.5120	1.0098

Table 6. The values of  $Nu_x/Ra_x^{1/2}$  and  $Sh_x/Ra_x^{1/2}$  for various values of  $\xi$  with N=1, Le=2, M=1, ND=1.

ξ	$Nu_x/Ra_x^{1/2}$	$Sh_x/Ra_x^{1/2}$
-2	1.0287	2.0300
-1	0.6430	1.1830
0	0.3732	0.5791
1	0.2004	0.2339
2	0.0982	0.0762